



Growth of high-quality single crystal of 30 at% Yb:YAG and its laser performance

Peizhi Yang^{a,*}, Peizhen Deng^b, Jun Xu^b, Zhiwen Yin^a

^aLaboratory of Functional Inorganic Materials, Shanghai Institute of Ceramics, Chinese Academy of Sciences, Shanghai 200050, People's Republic of China

^bShanghai Institute of Optics and Fine Mechanics, Chinese Academy of Sciences, Shanghai 201800, People's Republic of China

Received 8 February 2000; accepted 17 March 2000

Communicated by M. Schieber

Abstract

The Czochralski crystal growth of 30 at% Yb:YAG was reported. The growth parameters and annealing conditions were studied and the defects in Yb:YAG crystal were also investigated. The uniformity of 30 at% Yb:YAG was characterized using the absorption coefficient of Yb:YAG at 940 nm, and the laser performance of 30 at% Yb:YAG thin chip was demonstrated as well. The results show that Yb:YAG crystals with high doping level are potential candidates for compact, efficient thin chip lasers. © 2000 Elsevier Science B.V. All rights reserved.

PACS: 42.70.Hj; 81.10.Fg; 42.55.Rz

Keywords: 30 at% Yb:YAG; Crystal growth; Czochralski (CZ) method; Defects; Laser performance

1. Introduction

Recent advances in high-performance InGaAs laser diode with a wavelength between 0.9 and 1.1 μm have stimulated interest in diode-pumped Yb³⁺ lasers [1]. Yb³⁺ is a 4f¹³ ion, which possesses the simplest energy level structure, which has only two electronic states — the ²F_{7/2} ground state and the ²F_{5/2} excited state. In comparison with other rare-earth ions, since the next state, the 5d state, lies at approximately 100 000 cm⁻¹, some deleterious

effects such as excited state absorption (ESA) and upconversion are absent in Yb³⁺ lasers. So the Yb³⁺ ion is favorable for laser diode-pumped system [2].

Among the numerous Yb-doped oxide and fluoride crystals, Yb:YAG possesses many attractive laser characteristics, including high thermal conductivity and tensile strength of the host material, small quantum defect between the pump and the laser photons resulting in low thermal loading, broad absorption bands (about 18 nm at 940 nm) and long radiative lifetime of the upper laser level (1.3 ms). Especially, Yb:YAG shows high doping level possible without quenching, which is favorable for compact and miniature laser design. Thus, it is one of the most promising laser-active

* Corresponding author. Fax: + 86-021-62513903.

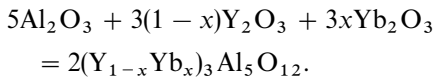
E-mail address: pzhyang@mail.sic.ac.cn, pzhyang@hotmail.com (P. Yang).

materials in near future [3]. Till now, pulsed, CW, Q-switched, passively model-locked femtosecond and multi-Watt laser actions have been achieved in LD-pumped Yb:YAG system. The highest CW output power was up to 434 W in diode-end-pumped Yb:YAG scheme [4].

In this article, high-quality Yb:YAG crystals with 30 at% doped concentration were grown by Czochralski method, and the growth parameters and annealing condition were also investigated. The defects in Yb:YAG were studied. The laser performance of 30 at% Yb:YAG thin chip ($5 \times 5 \times 0.2$ mm) was studied.

2. Crystal growth

Based on the Y_2O_3 - Al_2O_3 phase diagram, YAG ($Y_3Al_5O_{12}$) melts congruently at $1980^\circ C$. It is found that $Y_3Al_5O_{12}$ and $Yb_3Al_5O_{12}$ being completely miscible over a wide range because the yttrium and ytterbium garnets are isostructural with only about a 1.5% difference in unit-cell size and a $200^\circ C$ separation in their melting points [5]. As a result, most of the Yb substitutes the Y site in the dodecahedron. 30 at% Yb:YAG crystal was grown by the Czochralski (CZ) method along the $\langle 111 \rangle$ direction. Before being weighed to an accuracy of 10 mg, the raw materials of optical grade Al_2O_3 , Y_2O_3 , and 4N Yb_2O_3 were first dried at $200^\circ C$ to remove water. The composition of starting materials was chosen to be stoichiometric and the Yb^{3+} doping level was 30 at% according to the following reaction:



Uniform mixing was carried out in a ball mill coated with polyethylene. The mixture was pressed into rods and then sintered in a platinum crucible at $1200^\circ C$ for 24 h. The charge was then loaded into the irridium with a diameter of 70 mm and a height of 65 mm for crystal growth.

The optimal growth conditions were found to be as follows: rotation rate 10–20 rpm, pull rate 1 mm h^{-1} . The growth atmosphere was nitrogen or argon. The initial growth boundary in solid-melt



Fig. 1. 30 at% Yb:YAG crystal boule grown along the $\langle 111 \rangle$ direction.

was convex towards the melt so that the dislocations and impurity were reduced or eliminated. After that, the growth boundary became flat. In order to prevent the crystal from cracking, the crystal was cooled to room temperature slowly after growth. The crystal boule which was blue and free from crack, inclusions and precipitations was 32 mm in diameter and 100 mm in length, as shown in Fig. 1.

3. The defects

The main defects of Yb:YAG are color center, cores and stress striations caused by dislocation and facets. As-grown Yb:YAG crystal is blue, which demonstrated that there are Yb^{2+} and Re-F color centers [6]. The two absorption bands are located at wavelengths of 370 and 625 nm, respectively, as shown in Fig. 2. Yb^{2+} which caused the absorption band centered at 370 and 625 nm was attributed to Re-F color center. Yb^{2+} and Re-F color center in Yb:YAG are detrimental to the intrinsic spectroscopic performances of Yb:YAG. They degraded the Yb^{3+} intrinsic absorption at 900–1050 nm and the emission intensity at 1028–1060 nm and shortened the fluorescence lifetime of Yb^{3+} in YAG host.

The core, which is formed by the $\{211\}$ facet planes and the $\{110\}$ facet planes, and stress striations will cause Yb:YAG crystal optical heterogeneity. In order to eliminate Yb^{2+} , color center and reduce the core, stress striations, annealing

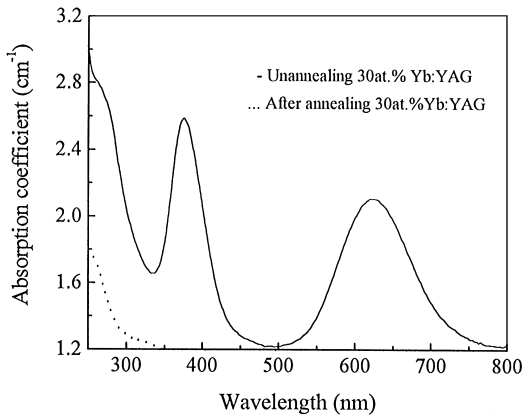


Fig. 2. The absorption spectra of 30 at% Yb:YAG crystal as-grown and after annealing.

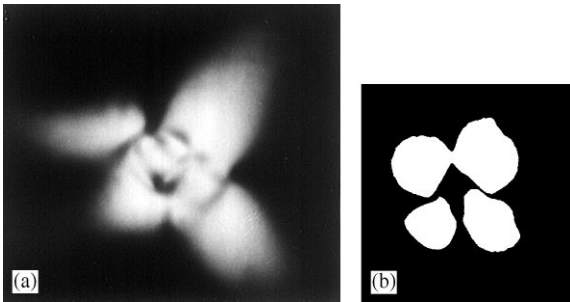


Fig. 3. (a) The stress-birefringence observed in a section of 30 at% Yb:YAG crystal as-grown and (b) after annealing.

processes were performed. The optimal annealing processing is as follows: in oxygen atmosphere Yb:YAG crystal boule was fired at 1600°C for 36 h, and then cooled to room temperature at a rate of 10°C h⁻¹. After annealing, the crystal changes from blue to colorless suggesting that the Yb²⁺ and color center was eliminated, and the area of core and stress striations is reduced, as shown in Fig. 3.

4. The uniformity

The absorption measurements were performed by a Perkin-Elmer spectrophotometer. After annealing, the Yb³⁺ concentration distributions along the crystal length and diameter direction were estimated according to the absorption spectra of Yb:YAG at 940 nm, shown in Figs. 4 and 5. From Fig. 4, we can see that there is a small

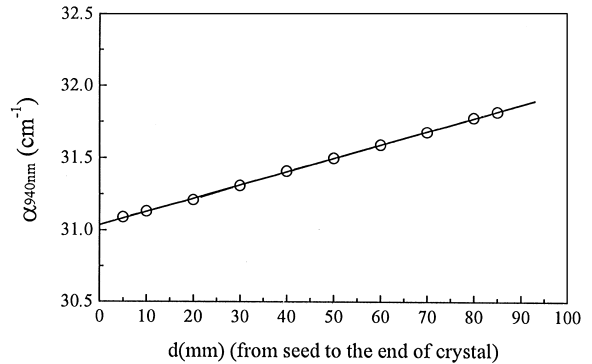


Fig. 4. The change of absorption coefficient of 30 at% Yb:YAG at 940 nm along the growth direction.

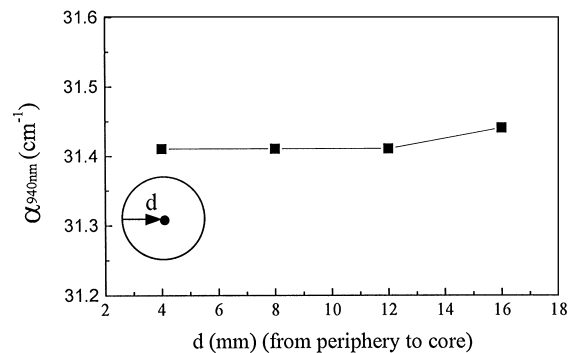


Fig. 5. The change of absorption coefficient of 30 at% Yb:YAG at 940 nm along the radius.

concentration gradient for Yb³⁺ ions along the length of crystal and that the distribution coefficient for Yb³⁺ in YAG must be close to unity. Fig. 5 shows that the concentration of Yb³⁺ along diameter direction is unity.

5. Laser performance

It is the purpose of growing 30 at% Yb:YAG to realize Yb:YAG microchip laser with high power and high efficiency, thus an efficient room-temperature 30 at% Yb:YAG microchip laser scheme was developed. The absorption and emission spectrum of Yb:YAG have shown that the peak at 940 nm is the strongest absorption feature and the broad laser transition is at 1.03–1.055 μm [7]. The Ti:sapphire laser with emitting wavelength of 940 nm was adopted as the pump source in the laser

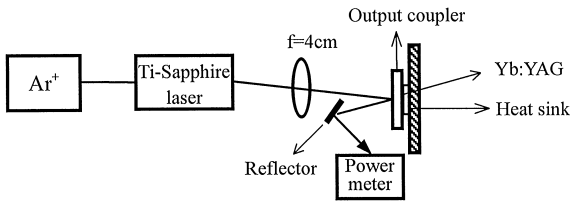


Fig. 6. Experimental setup of the Ti:sapphire laser pumped Yb:YAG thin chip laser.

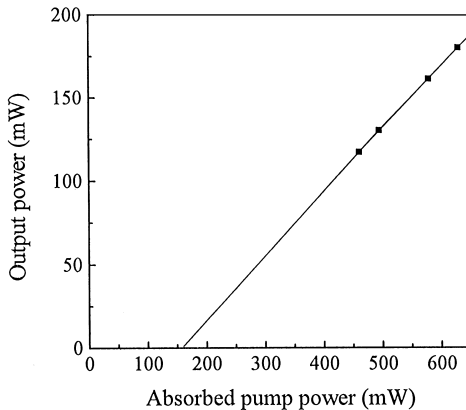


Fig. 7. Room-temperature output power versus absorbed pump power of Ti:sapphire pumped 30 at% Yb:YAG ($5 \times 5 \times 0.20 \text{ mm}^3$).

experiment. Using delicate select technique, laser chip can be cut out of the crystal free from cores and facets. The experimental setup is shown in Fig. 6. Laser resonator was formed from flat–flat cavity. The Ti:sapphire laser beam (beam diameter approximately 4 mm) is focussed with a focal length of about 40 mm onto the front side of the cavity lens. The front side is high transmission for the pump wavelength at 940 nm and high reflectivity for the laser wavelength at 1.03–1.055 μm . The crystal chip ($5 \times 5 \times 0.20 \text{ mm}^3$) was AR coated for both wavelengths on the front side and HR coated for both wavelengths on the back side, which was mounted on a heatsink. The HR-coated back side of the crystal acting as folding mirror and flat mirror form a resonator. A typical plot of the laser output power at 1.053 μm versus the absorption pump power for output coupler reflectivity of 98.82% is shown in Fig. 7. CW output power of 180 mW was obtained with an absorbed pump power of 629 mW at room temperature, slope

efficiency is 38%. High output power and higher efficiency should be possible with more optimized output coupler reflectivity.

6. Conclusion

The Yb:YAG crystal doped with 30 at% Yb^{3+} was grown by the CZ method. The crystal boule was 32 mm in diameter and 100 mm in length. The optimal growth parameter and annealing conditions were presented. Annealing was performed in oxygen at 1600°C for 36 h, and then the crystal was cooled to room temperature at a rate of 10°C h⁻¹. The color center, core, stress striations in Yb:YAG were studied and it was demonstrated that annealing can eliminate the color center and reduce the defects of core and stress striations. The absorption spectra show that the concentration of Yb^{3+} along the growth axis and the radius is near unity. The 30 at% Yb:YAG thin chip ($5 \times 5 \times 0.2 \text{ mm}$) laser operating at 1.053 μm pumped by Ti:sapphire laser was developed and 180 mW of CW output power was obtained for an absorbed pump power of 629 mW. The slope efficiency was 38% and the extrapolated threshold power is 160 mW.

Acknowledgements

This work was supported by National Natural Science foundation of China under project 69578026 and National 863-416 Foundation of China.

References

- [1] P. Lacovara, H.K. Choi, C.A. Wang, R.L. Aggarwal, T.Y. Fan, *Opt. Lett.* 16 (1991) 1089.
- [2] T.Y. Fan, *IEEE J. Quantum Electron.* 29 (1993) 1457.
- [3] A. Giesen, H. Hügel, A. Voss, *Appl. Phys. B* 58 (1994) 365.
- [4] C. Bibeau, R.J. Beach, S.C. Mitchell et al., *IEEE J. Quantum Electron.* 34 (1998) 2010.
- [5] A.R. Reinberg, L.A. Riseberg, R.M. Brown et al., *Appl. Phys. Lett.* 19 (1971) 11.
- [6] H.B. Yin, P.Z. Deng, F.X. Gan, *J. Appl. Phys.* 83 (1998) 3825.
- [7] P.Z. Yang, P.Z. Deng, J. Xu et al., *Acta Opt. Sinica* 19 (1999) 132 (in Chinese).